

# Design and performance of an astrometric beam combiner for space interferometry

R. P. Korechoff, S. B. Shaklan, Y. Lin, R. D. Bartos, D. M. Moore  
Jet Propulsion Laboratory, California Institute of Technology  
Pasadena, California 91109

## ABSTRACT

This paper describes the design and performance of a brassboard astrometric beam combiner. The beam combiner was developed as part of the JPL Interferometry Technology Program (ITP). The purpose of this program is to test out design concepts in hardware that will eventually be used for the Space Interferometry Mission (SIM). The label brassboard implies that the beam combiner is flight like in terms of fit and function. The beam combiner met its design performance except for fringe visibility. Although it has not been environmentally tested as an assembly, the beam combiner was designed to survive the appropriate thermal and vibration tests.

**Keywords:** interferometry, beam combiner

## 1. INTRODUCTION

The Space Interferometry Mission (SIM), currently being developed at JPL, is expected to revolutionize the field of astrometry. The SIM instrument will measure the relative positions of stars with unprecedented accuracy, namely  $4 \mu\text{as}$  for wide angle astrometry and  $1 \mu\text{as}$  for narrow angle astrometry. This quantum jump in astrometric capability (more than two orders of magnitude improvement over Hipparcos) implies the need for technology development of almost every critical SIM subassembly associated with the handling of the starlight and metrology beams. In order to meet these technology challenges, JPL has instituted a three-tier development program. The first step is the design and testing of brassboard versions of key components and subassemblies. This stage is being carried out under the Interferometry Technology Program (ITP). The second step is a series of testbeds including one that is essentially an engineering model of the full instrument. The final step is the construction of the flight instrument. Clearly, the purpose of the first two steps is to reduce the risk associated with various components, subassemblies, and subsystems before they are implemented in the flight instrument.

In this paper we describe the design and performance of the brassboard astrometric beam combiner which was an ITP development. In this case, the term brassboard means that the hardware must meet the flight requirements with respect to packaging, environmental testing, and reliability. In the area of performance, some flight requirements were modified to account for the fact that the detector was commercial grade and not all the optical components met flight specifications because of budget and schedule constraints.

The brassboard beam combiner, shown in Fig. 1, is the heart of the interferometer. The starlight beams from each arm of the interferometer are directed to the beam combiner where they are interfered. The interfered light is detected as both a composite white light fringe and as a spectrally dispersed fringe. In addition, the beam combiner provides feedback information to correct wavefront tilt and beam shear. Finally, the beam combiner optics must accommodate the internal metrology beams which are launched through the beam combiner beamsplitter into each arm of the interferometer. These metrology beams, at  $1.3 \mu\text{m}$ , are spectrally separated from the starlight and are tagged by their polarization. The sections that follow describe how these various functions are performed in the beam combiner.

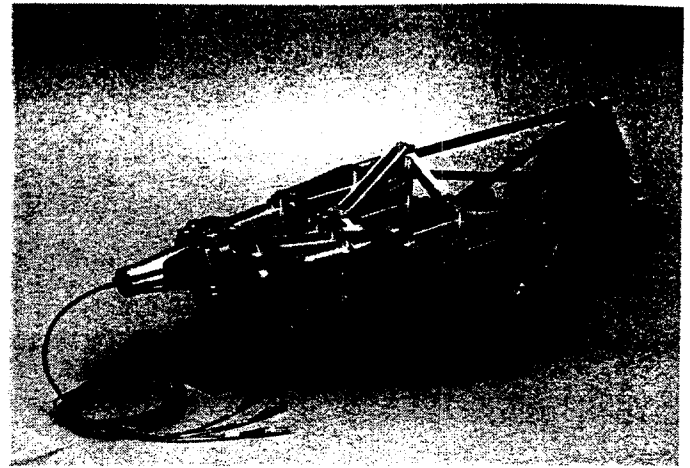
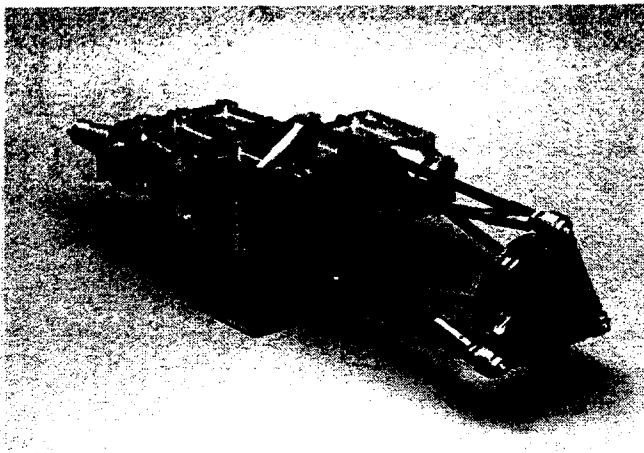


Figure 1. Front and back views of the SIM brassboard beam combiner.

## 2. ARTIFICIAL STAR

The artificial star provides the illumination for the beam combiner. The illumination can either be narrow band (helium-neon laser) or broadband (incandescent source). The principal functional requirements of the artificial star are to collimate the light source and divide the collimated beam into two beams of approximately equal intensity. An optical layout of the artificial star is shown in Fig. 2.

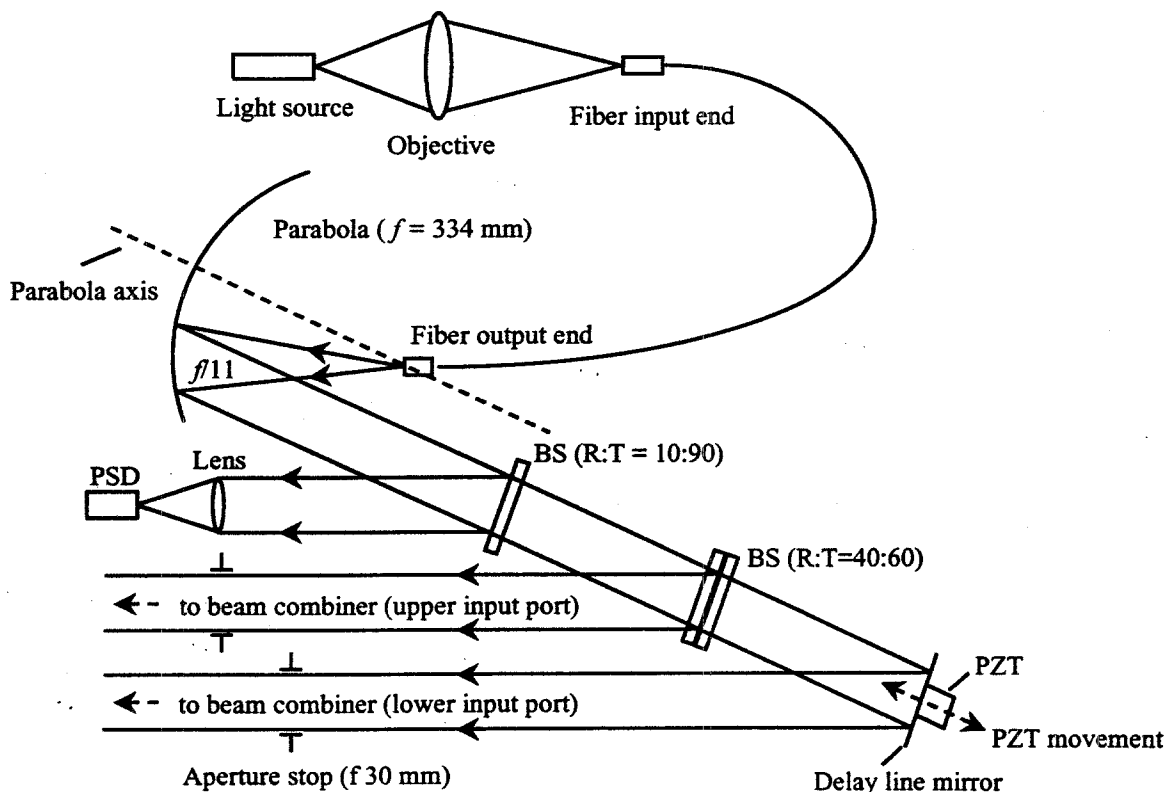


Figure 2. Optical layout for beam combiner artificial star.

The collimation is accomplished by focusing the light source (narrow or broad band) on the end of an optical fiber with a microscope objective. The other end of the fiber is located at the on-axis focal point of a parabolic mirror. The fiber is tilted to illuminate a decentered portion of the parabola producing an unobscured, collimated beam. The collimated source then passes through a beamsplitter that picks off

about 10 percent of the incident light which is focused on a position sensitive detector (PSD). Unintentional displacements of the fiber end from the parabola focal plane, which add a power term to the source beam, are thus detected at the PSD. The dispersion through the PSD beamsplitter is not a concern because the optical path delay is a common mode effect.

The transmitted portion of the beam passes through another beamsplitter which has a reflection/transmission ratio of approximately 50/50. This ratio is critical because it determines the relative intensity in each interfering arm; fringe visibility is maximized when the relative arm intensity ratio is unity. The light reflected by this beamsplitter becomes the input to what we have designated, for convenience, the beam combiner upper port. The light transmitted by the beamsplitter is reflected by a flat mirror that directs it into the beam combiner lower port. Before entering the beam combiner each input beam passes through a 30-mm diameter aperture.

The position of the flat mirror that reflects light into the beam combiner lower port can be stepped along the beam direction. The mirror's position is varied by PZT actuators in steps of 40 to 200 nm with a total stroke capability of 21  $\mu\text{m}$ . The purpose of this actuator is to change the optical path difference (OPD) between the two beams input to the combiner in a controlled manner. The mirror translation as a function of voltage applied to the PZTs was calibrated from the dispersed fringe data.

### 3. BEAM DIVISION BY FUNCTION

As described above, the beam combiner must perform a number of different functions simultaneously. The key to accomplishing these various functions is the division of the input beams into three zones with each zone dedicated to a different function. This beam division is illustrated in Fig. 3.

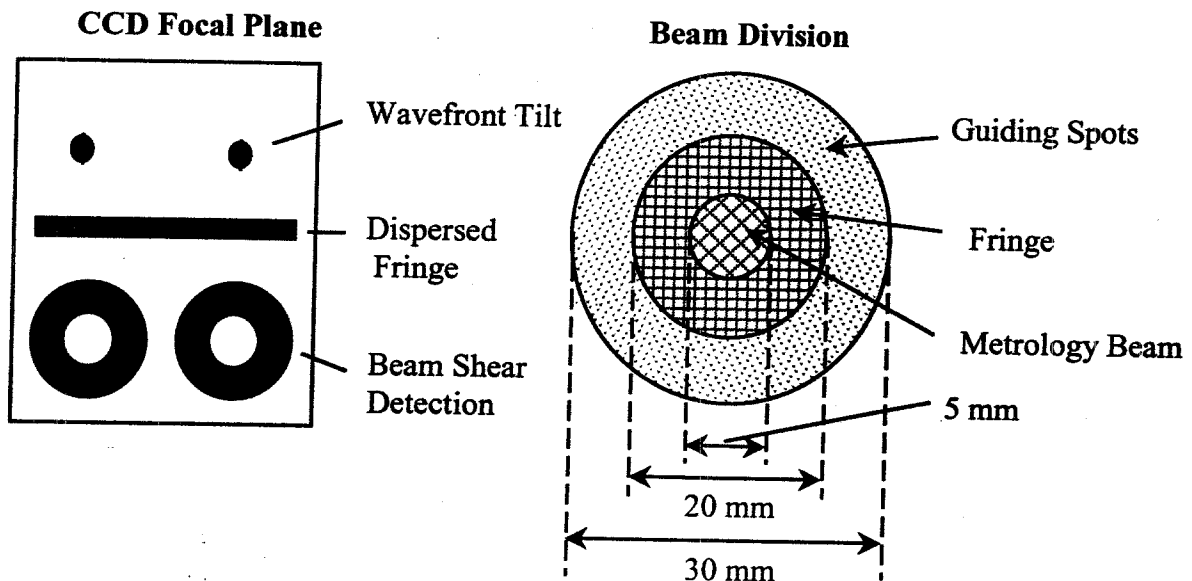


Figure 3. The input beam is divided into three zones according to function. The guiding zone light appears as focused and defocused images at the CCD as explained in the text. The fringe zone appears as a dispersed fringe. See Fig. 6 for photo of actual CCD frame.

The inner 5-mm diameter of the beam is given over to the internal metrology beam. That is, the starlight in this region of the input beam is not utilized; this represents only about a 3 percent loss. The annular region from 5 to 20 mm (designated as the inner annulus), representing about 42 percent of the input light, is used to form fringes. The annular region from 20 to 30 mm (designated as the outer annulus), representing about 56 percent of the input light, is used to correct wavefront tilt and beam shear. Although it may appear that

an inordinate amount of light has been consigned to beam diagnostics, as opposed to fringe formation, the ratio of the diameters of the inner and outer annuli were optimized based on read noise, photon statistics, and filtering for guiding. Furthermore, for reasons explained in Sec. 4, it is not desirable for the fringe light to be the outer annulus.

Also shown in Fig. 3 is the appearance of each region of the input beams on the beam combiner detector<sup>1</sup>. The diagnostic spots indicating wavefront tilt and beam shear come from the outer annulus while the dispersed fringe is produced by the inner annulus. The diagnostic spots are not interfered thus producing one spot of each type from each input arm to the beam combiner. The dispersed fringe obviously contains the light from both arms. The details concerning the generation and interpretation of these images are given in the next section.

#### 4. BEAM COMBINER OPERATION

The optical layout of the beam combiner is shown in Fig. 4. The two input beams propagate along virtually identical optical paths (the upper input beam has an additional reflection) up to the interfering beamsplitter. The first component encountered by the input light is a glass window containing a 5-mm diameter polarizing disk bonded on the window and centered with respect to the beam. The polarizers insure that the internal metrology beams are tagged by the appropriate polarization state. As mentioned above, the starlight in this central region is not used. The next component is a constant deviation prism (#1). This prism introduces a tilt of approximately 260 as in magnitude to the outer annulus of each input beam. The direction of the tilt can be varied by rotating the prism. By properly positioning the prisms, the images of the two outer annuli are spatially separated by a known amount in the beam combiner focal plane. The inner annulus passes through a hole in the prism and thus picks up no additional tilt.

Both the polarizers and the constant deviation prisms are held in place by optical windows rather than spiders. Each method has good and bad features. Diffraction from spiders produces extended images at the beam combiner detector. Furthermore, because multiple spiders would be required, the alignment of the spiders relative to one another becomes an issue. For these reasons optical windows were chosen to hold various elements. However, passing the starlight through a transmissive element means that the two input beams can no longer be made to traverse equal optical paths at all wavelengths. Note that if the guiding and fringe annuli were reversed, the fringe forming light would have to pass through two windows, one holding the polarizers and one holding the constant deviation prism.

After constant deviation prism #1, the two input beams are combined at the beamsplitter. The beamsplitter is a sandwich design with equal thicknesses of fused silica (within 0.1 mm) surrounding a dielectric, multi-layer coating. The outer faces of the beamsplitter have an anti-reflection coating which is optimized for the operating angle of incidence, namely 15°. Since each input beam is both transmitted and reflected by the beamsplitter, two interfered beams (inner annuli) and two diagnostic beams (outer annuli) are generated. All the beams generated by the beamsplitter are eventually imaged by a parabolic mirror on either a CCD or an avalanche photo-detector (APD). Although a discussion of the SIM internal metrology scheme is not a part of this paper, it is important to point out that the beamsplitter coating must also divide the 1.3  $\mu\text{m}$  metrology beam; however, the transmission/reflection ratio is not as critical for the metrology beam.

The upper interfered beam inner annulus in Fig. 4 passes through a zero deviation prism<sup>2</sup> which is then imaged as a dispersed fringe on the CCD (see Fig. 3 or 6). The upper interfered beam outer annulus passes through two windows holding the zero deviation prism and is focused as diffraction limited spots on the CCD. The guiding spots are located at the CCD on a circle with a radius of approximately 14 pixels as a result of the 260 as tilts introduced to the outer annuli wavefronts. The exact position of the guiding spots

<sup>1</sup> The arrangement of the various images in the brassboard detector differs somewhat from the illustration in Fig. 3.

<sup>2</sup> Zero deviation prism means zero deviation at a particular wavelength only. In this case, that wavelength is approximately at the center of the spectral band of interest.

on this circle is determined by the clocking of the two constant deviation prisms #1. Once the nominal location of each guiding spot is established, deviations of the centroid of the spot from that position are an indication of the wavefront tilt of the interfered portion of the starlight.

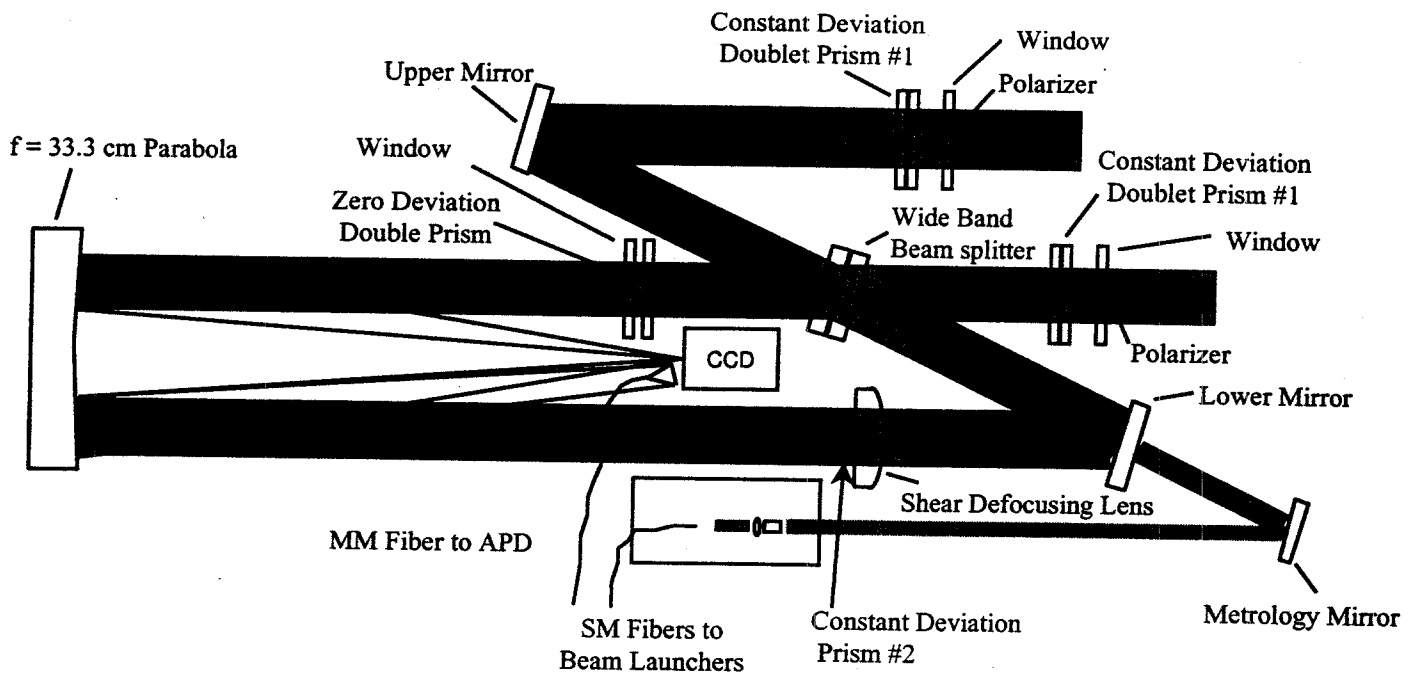


Figure 4. Optical layout of the SIM brassboard beamcombiner.

The Airy disk of the guiding spots is subpixel -- one half to two-thirds of a pixel depending on the wavelength. In order to achieve detection of small tilts the guiding spots must be centered on the intersection of four pixels so that the CCD functions as a quad cell. This is accomplished by rotating the guide spot images until they are parallel to a row of pixels and separated by an integral number of pixels. Then the parabola is tilted to simultaneously move the guide spot images to the corners of four pixels. The outputs from these simulated quad cells are feedback to the fast steering mirrors to remove the tilt in each arm. In this manner the wavefronts of the interfering beams are kept parallel. This wavefront correction function was never tested with the brassboard beam combiner.

The lower interfered beam inner annulus passes through a constant deviation prism #2 as shown in Fig. 4. This prism introduces a wavelength-independent tilt to the interfered starlight so that the parabola will form an image at a position in the focal plane that is displaced from the dispersed fringe. However, before this focused light actually reaches the CCD, it is reflected by a small fold mirror to a fiber which transmits the interfered light to an APD. Hence, half the interfered light is detected as a dispersed fringe and half is detected as a spectrally composite (white light) fringe. The dispersed fringe provides more information about the relative pathlength difference between the two arms of the interferometer but will have a poor signal-to-noise ratio for dim sources. In these cases the APD will provide fringe information which is used to control pathlength. The dispersed fringe is also utilized in the imaging mode where each spectral interval represented by a pixel contributes a point to the u-v plane.

The remaining beam to be discussed is the lower interfered beam outer annulus. These wavefronts carry the same tilts as their counterparts in the upper beam. However, this annulus passes through a lens that performs two functions. First, it introduces a wavelength-independent tilt which spatially displaces the image of these spots from those used for wavefront tilt information. Second, it adds power to the wavefront so the spots are defocused at the CCD. Enough power is added so that the image formed at the CCD shows

the starlight distribution in the pupil which is an annulus (see Fig. 3 or 6). Asymmetries in this intensity distribution indicate beam shear although no information is provided concerning which optical element (or elements) is responsible for the shear.

## 5. MECHANICAL DESIGN

The goal of the beam combiner mechanical design was to produce a compact, light weight housing capable of maintaining the position and orientation of the various optical components subject to expected launch vibration and on-orbit temperatures swings of  $\pm 10^\circ \text{C}$ . In addition, it was desired to be able to adjust all the optical components without disassembling the housing. Furthermore, these adjustments should be done without shimming which is time consuming and leaves open to possibility of slippage. This goal was accomplished with a structure consisting of four main pieces: main housing, secondary housing, metrology bulkhead, and hexapod truss. These pieces are shown in an exploded view of the beam combiner in Fig. 5. The weight of the beam combiner housing alone is about 4.5 kg and 6.4 kg including all the optics and the internal metrology beam launcher.

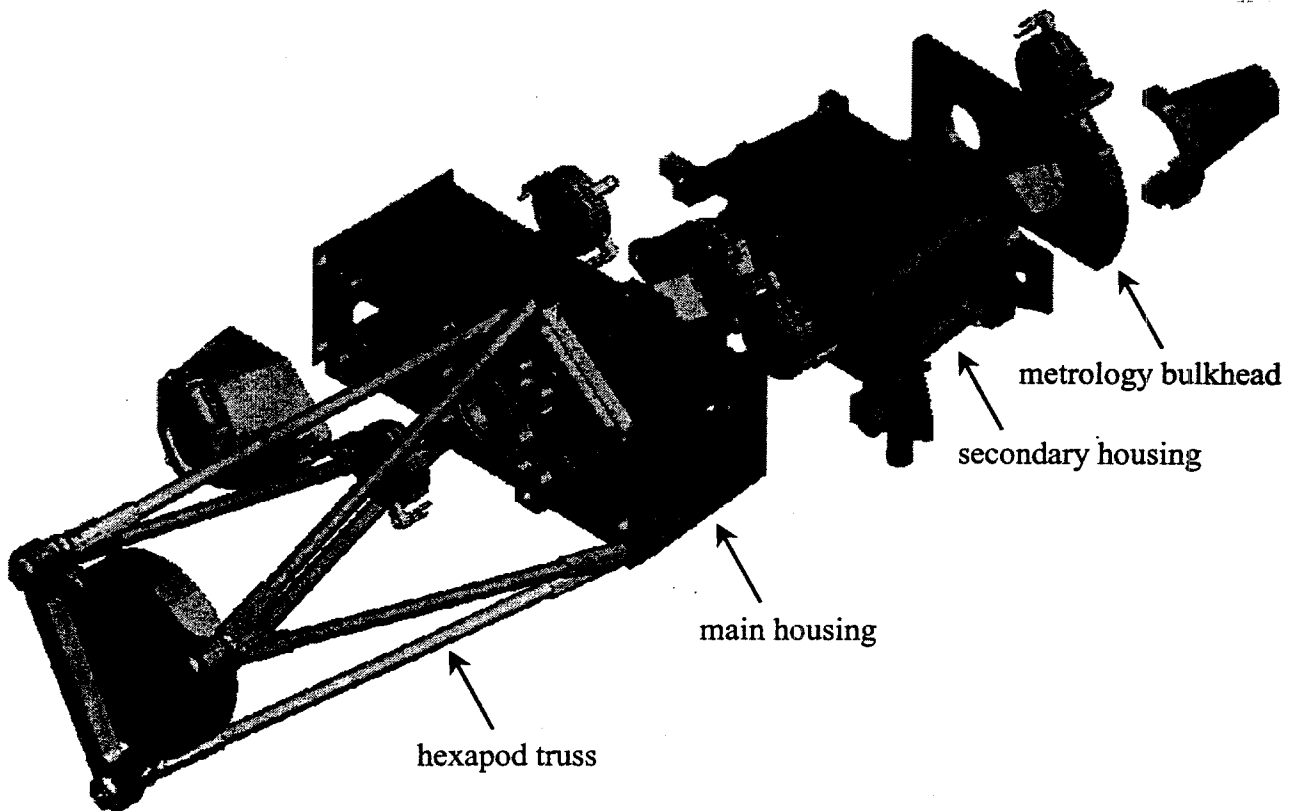


Figure 5. Exploded view of the beam combiner showing mechanical interfaces.

The main housing is a box beam construction with the structure axis perpendicular to the optical beams. Apertures have been cut in the side walls at six locations to allow passage of the starlight and metrology beams. Eight optical components and the CCD are mounted to the main housing to maximize the alignment stability of the beam combiner. The secondary housing is also a box beam but its structure axis is parallel to the optical beams. Its main function is to act as a stable spacer between the metrology bulkhead and the main housing. It also contains a mounting flange for the internal metrology beam launcher. The metrology bulkhead provides a mounting location for three optical components and a conical adapter that contains a piezo actuator for steering the internal metrology beam after it leaves the launcher. The three structural

elements discussed so far hold all the optics except for parabolic mirror. All the light in these three sections of the beam combiner is collimated thus effectively eliminating thermal expansion as a dominant issue. Consequently, these structural elements were fabricated of 7075-T7351 aluminum alloy taking advantage of this materials good weight to stiffness ratio and ease of machining.

The fourth main structural component is the hexapod truss which is required to maintain a stable geometry between the main housing and the parabolic focusing mirror. Since this is the portion of the beam combiner where collimated light becomes a converging beam, thermal expansion is an important consideration. For this reason the hexapod truss was constructed with graphite/cyanate ester tubular members and titanium end fittings. Graphite/cyanate ester was chosen over graphite/epoxy because it is less hydroscopic by an order of magnitude.<sup>3</sup>

Two types of mounts are utilized for the various optical components, namely tip-tilt-piston (TTP) and rotatable. The TTP mounts represent a new genre of mount designed specifically to satisfy the requirement for a highly stable yet readily adjustable mount. The TTP mounts were used in the beam combiner to hold the upper input beam fold mirror, the beamsplitter, and the mirror following the beamsplitter. The mounts are machined from aluminum alloy but the mirrors are attached to the adjustable cells by three bipods to avoid transmitting thermal distortions to the optics. The bipods for the mirrors are fabricated from titanium whose CTE closely matches that of the BK7 mirror substrates. The fused silica beamsplitter is bonded to three Invar bipods which, in turn, are bolted and pinned to the mirror cell. The cells are machined integral to their mounting structures such that they bolt directly to the housings at the proper angle (15° angle of incidence) and position.

The TTP mounts contain no actuators. The cells that contain the optics are held at three points by opposing spherical washers. The washers are accessible without removing any parts and can be translated along a linear screw with a wrench. The full range in tip/tilt is approximately  $\pm 1^\circ$ . Operation with the mounts demonstrated that they were adjustable to 0.2 as in less than 20 minutes. The TTP mounts were put through extensive environmental testing. The tip/tilt orientation of the mounts changed by less than 1 as after undergoing a 3-minute, full-launch level, random vibration test. The tip/tilt stability was 1.5 as after thermal vacuum testing over the temperature range 10 - 30°C.

Rotational adjustment is required for annular wedges, polarizer support windows, prisms and the shear defocus lens. In addition, translation is required for the annular wedges and polarizer support windows. These optics are fabricated from BK7 glass thus mandating the use of titanium for the mirror cells. The thermal expansion mismatched between the mirror cell and the optic is handle by flexures which provide a soft radial compliance. The translatable versions of the rotatable mirror mounts use four screws to move the mirror cell; when the optic is correctly positioned the screws are bonded into place thus insuring translational stability.

## 6. PERFORMANCE

The qualitative performance of the beam combiner is shown in Fig. 6 which is a frame taken from the beam combiner CCD. As described in Sec. 4, the detector shows a pair of wavefront tilt guiding spots, a pair of defocused spots measuring beam shear, and a dispersed fringe. The positions of the images are not identical to the design shown in Fig. 3 due to a fabrication error in the zero deviation prism which moved the dispersed fringe away from the guiding and shear spots. The fringe shows the pronounced non-uniformity in the source spectral radiance. The shear spots in Fig. 6 show good geometrical symmetry but a distinct asymmetry in illumination. Since the shear spots represent the intensity pattern in the pupil, one explanation for the uneven intensity is asymmetry in the input beams. However, horizontal and vertical scans across the input beams with a 1-mm square detector showed good radial symmetry. A more likely explanation is a slight misalignment of optical components. The beam combiner depends on precise

---

<sup>3</sup> The structure holding the primary and secondary mirrors for the Hubble Space Telescope was made of graphite/epoxy. This structure is still shrinking (drying) after eight years on-orbit.

translational alignment of components so that the annular zones passes through each element are well registered.

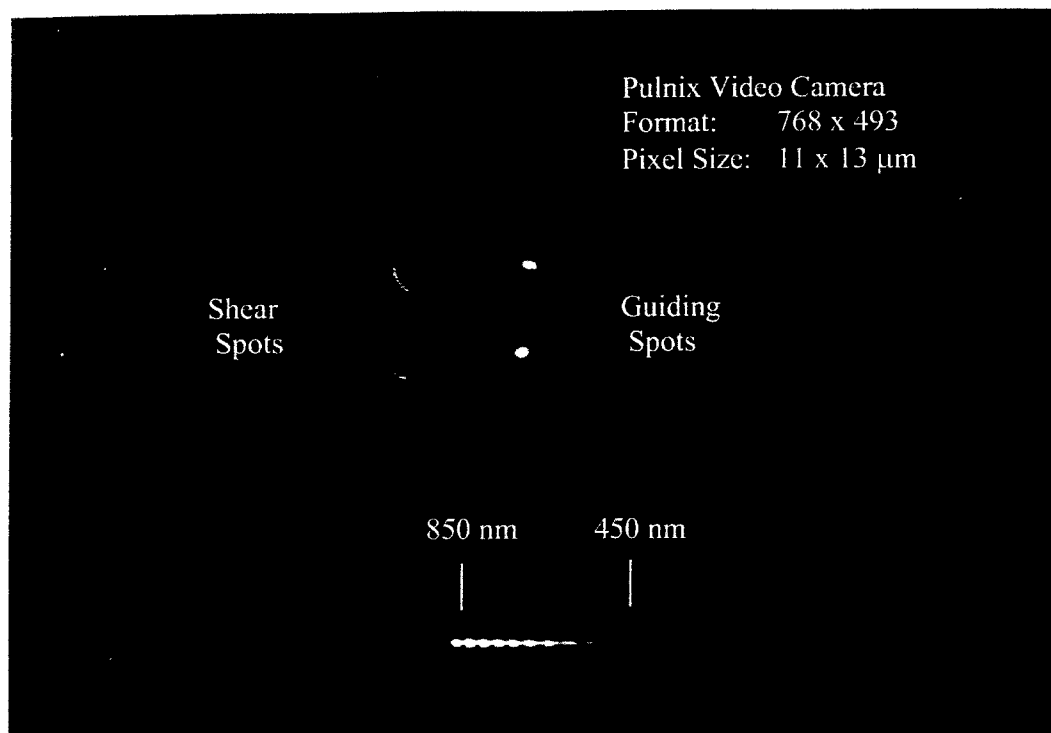


Figure 6. Beam combiner CCD frame showing guiding

Table 1. Beam combiner performance for selected parameters

Parameter	Design	Measured
Fringe visibility (combiner only)	0.85	0.33 - 0.61
Guiding spot throughput (including geometry)	0.14	0.16
Fringe throughput (including geometry)	0.20	0.24
Spectral resolution	$\lambda/100$	$< \lambda/200$
Fringe dispersion linearity	$< 5\%$	$< 5\%$ (550-800 nm) $> 5\%$ ( $> 800$ nm)
OPD tuning range	18 $\mu\text{m}$	21 $\mu\text{m}$
Beamsplitter T/R (500 - 900 nm)	$< 60/40$	$< 60/40$

A quantitative assessment of the beam combiner's performance is shown in Table 1 for several selected parameters. The only parameter failing to meet the design specification was the fringe visibility. Fringe visibility is affected by a number of parameters including relative intensity in the interfering beams,



polarization mismatch, wavefront tilt, wavefront errors, beam shear, and stray light. In trying to determine the source of the degraded visibility, we note that the other parameters given in Table 1 met or exceeded their design performance. The combination of these other parameters covers many aspects of the beam combiner optical components and thus indicate no abnormal behavior. At this time the degradation in the fringe visibility is not understood.

## **7. ACKNOWLEDGMENT**

This work was carried out by the Jet Propulsion Laboratory, California Institute of Technology, under contract with the National Aeronautics and Space Administration.